PHYSICAL REVIEW B **79**, 060201(R) (2009)

Relaxation kinetics and mechanical stability of metallic glasses and supercooled melts

S. G. Mayr*

I. Physikalisches Institut, Georg-August-Universität Göttingen, Friedrich-Hund-Platz 1, 37077 Göttingen, Germany

(Received 23 October 2008; revised manuscript received 17 December 2008; published 13 February 2009)

Metallic glasses are characterized by a rather complex viscoelastic response and the occurrence of the glass transition, while the atomistic origins are still poorly understood. Using a realistic CuTi model glass we employ global and local elasticity tensors for a thorough analysis of relaxation kinetics and mechanical stability. We obtain strong indication that (i) α relaxation is governed by an underlying process (identified as slow β relaxation) which resembles diffusion in its temperature dependence, (ii) glasses reveal intrinsic mechanical instabilities, which are closely linked to collective shear events within shear transformation zones, and (iii) glass transition can be understood as a percolation transition of mechanically unstable regions.

DOI: 10.1103/PhysRevB.79.060201 PACS number(s): 61.43.Fs, 62.10.+s, 64.70.pe, 83.50.−v

As already pointed out by Born[1] almost 70 years ago, the elasticity tensor is a key quantity to characterize the stability of condensed matter with respect to strain, e.g., to discriminate solids from liquids by the failure of liquids to sustain shear strain. Clearly this concept is also suitable for the liquid-glass transition, which is characterized by the onset of viscous flow.

When dealing with glasses, care, however, has to be taken due to (i) viscoelastic properties[2] and (ii) dynamical heterogeneities (see, e.g., Ref. 3 for a review). Basically, (i) constitutes an observation time dependence of the response to an applied disturbance and manifests itself, e.g., in strain-rate-dependent mechanical properties[4] or in the heating rate dependence of the glass transition itself.[5] The latter can be unveiled by observations on multiple times scales, which poses the main challenge—both experimentally and from a simulation point of view. Indications for (ii)—although initially not identified as such—date back to the first observations of a stretched exponential (Kohlrausch[6]) decay of the relaxation functions in amorphous systems.[3] Strong corroboration for spatial mechanical heterogeneities [so-called "shear transformation zones" (STZs)] originates from analytical and computational model systems[7–11] as well as compilations of experimental data.[12] Given that elastic constants are directly linked to system structure and dynamics,[13] STZs are certain to leave their fingerprints directly on elastic properties. Vice versa, this suggests local elastic properties as ideal probe to track down STZs—in experiments and atomistic computer simulation.

In our present study we employ massively parallel classical molecular dynamics (MD) simulations on a $Cu_{50}Ti_{50}$ model glass with the aim of clarifying the spatiotemporal hierarchy of processes, which govern the mechanical response of glasses and the glass transition. Employing a realistic embedded atom method (EAM) potential[14] for CuTi (Ref. 15) in a self-written massively parallelized MD code, highly relaxed amorphous a−$Cu_{50}Ti_{50}$ cells with $\approx 3.5 \times 10^4$ particles each were prepared by quenching from melt (6000 K) with rates of 0.1 K/ps, subsequent annealing around the glass transition temperature ($\gtrsim 0.2$ μs at 600 K) and final approach of the desired temperature, all under isobaric ($\sigma_{ii}=0$; $i=1,2,3$) conditions in a rectangular simulation box. Temperatures and pressures were controlled with Nose-Hoover[16,17] thermostats and Berendsen barostats,[18] respectively. Amorphicity was verified by calculating the radial/angular distribution functions, by monitoring the onset of viscous flow under applied shear stress at T_G, as well as by calorimetry. The global elasticity tensor, C_{ijkl}, of the total cell is calculated in an (T,h,N) ensemble, following the original fluctuation formalism of Ray *et al.*,[13] as adapted for EAM potentials.[19,20] To address local properties, the simulation box is subdivided into a cubic raster; C^{λ}_{ijkl} within each subcell, λ, is computed by following a formalism proposed by Lutsko[21,22] which had been generalized for binary EAM potentials in the present work. Based on the original EAM formalism,[14] we assume, that ρ_α, ρ^T_α, Γ_α, and $\phi_{\alpha\beta}$ denote the atomic electron density of α, the total electron density in the location of α, embedding energy and pair interaction, respectively. The elasticity tensor, C^{λ}_{ijkl}, is then calculated as sum of so-called Born terms (B^{λ}_{ijkl}) as well as fluctuation (F^{λ}_{ijkl}) and kinetic (K^{λ}_{ijkl}) contributions

$$C^{\lambda}_{ijkl} = \underbrace{\langle B1^{\lambda}_{ijkl}\rangle + \langle B2^{\lambda}_{ijkl}\rangle + \langle B3^{\lambda}_{ijkl}\rangle}_{B^{\lambda}_{ijkl}} + F^{\lambda}_{ijkl} + K^{\lambda}_{ijkl}. \tag{1}$$

Here $\langle\cdot\rangle$ denotes an average over observation time for an ensemble of systems initially residing in different metastable states (excluding transient states). Defining $\zeta^{\lambda}_{\alpha\beta}$ as that fraction of $r_{\alpha\beta}$ that lies within box λ, we obtain

$$B1^{\lambda}_{ijkl} = \frac{1}{2V^{\lambda}} \sum_{\substack{\alpha,\beta \\ \alpha\neq\beta}} \left(\phi''_{\alpha\beta} - \frac{\phi'_{\alpha\beta}}{r_{\alpha\beta}}\right) \frac{r_{\alpha\beta i}\, r_{\alpha\beta j}\, r_{\alpha\beta k}\, r_{\alpha\beta l}}{r^2_{\alpha\beta}} \zeta^{\lambda}_{\alpha\beta}, \tag{2}$$

$$B2^{\lambda}_{ijkl} = \frac{1}{V^{\lambda}} \sum_{\substack{\alpha,\beta \\ \alpha\neq\beta}} \Gamma'_{\alpha} \left(\rho''_{\beta} - \frac{\rho'_{\beta}}{r_{\alpha\beta}}\right) \frac{r_{\alpha\beta i}\, r_{\alpha\beta j}\, r_{\alpha\beta k}\, r_{\alpha\beta l}}{r^2_{\alpha\beta}} \zeta^{\lambda}_{\alpha\beta}, \tag{3}$$

$$B3^{\lambda}_{ijkl} = \frac{1}{2V^{\lambda}} \sum_{\substack{\alpha,\beta,\gamma \\ \beta\neq\alpha \\ \gamma\neq\alpha}} \Gamma''_{\alpha}\, \rho'_{\beta}\, \rho'_{\gamma} \frac{r_{\alpha\beta i}\, r_{\alpha\beta j}\, r_{\alpha\gamma k}\, r_{\alpha\gamma l}}{r_{\alpha\beta}\, r_{\alpha\gamma}} (\zeta^{\lambda}_{\alpha\beta} + \zeta^{\lambda}_{\alpha\gamma}), \tag{4}$$

while F^{λ}_{ijkl} and K^{λ}_{ijkl} are given in Ref. 21. It is interesting to note within this context that B^{λ}_{ijkl} describes the isoconfigura-

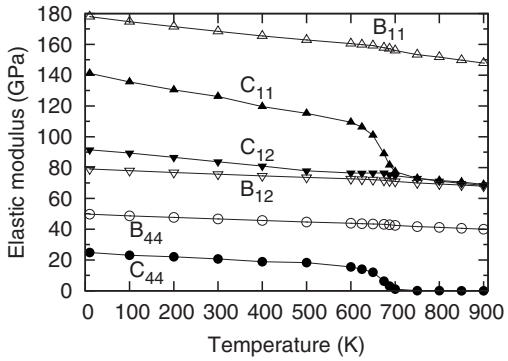

FIG. 1. Temperature dependence of global elastic properties of a fully relaxed amorphous CuTi simulation cell (observation time: 1.0 ns).

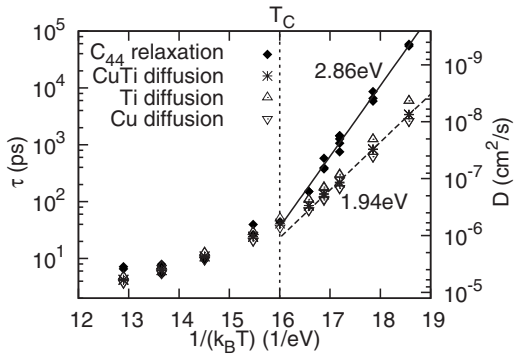

FIG. 3. Relaxation times τ in comparison with the diffusion constants at different temperatures. $T_C \approx 725$ K correspond to the critical temperature of the mode-coupling theory.

tional shear modulus and is found to be the largest positive contribution in Eq. (1) for the system investigated. F^{λ}_{ijkl} describes softening due to reconfigurations and is found to be particularly important in the liquid state, while K^{λ}_{ijkl} is two orders of magnitudes smaller than the other terms within the present studies. Figure 1 shows three major components of the elasticity tensor, C_{ij} for an observation time of 1.0 ns, as well as the corresponding Born terms, B_{ij}, using Voigt notation. The pronounced drops of C_{11} toward C_{12} and of C_{44} toward zero in the range of 600–700 K indicate vanishing shear moduli for $T \geq T_G \approx 687.5$ K. It is also intriguing to point out that the Born terms do not reveal any significant anomalies when increasing the temperature beyond T_G. Noting that B_{ij} is only (but strongly) dependent on the structure, this clearly indicates that *no* significant structural changes occur at T_G, thus corroborating its kinetic nature.

The latter aspect is investigated in detail in Fig. 2, which shows a dramatic decrease in the shear modulus, C_{44}, with increasing time around T_G. Detailed inspection of the exact shape of $C_{44}(t)$ unveils a stretched exponential, Kohlrausch type of decay with $\beta=0.5$ for all temperatures investigated.[23]

In the following we aim to address the stretched exponential α relaxation in more detail. Figure 3 shows an Arrhenius plot of the corresponding relaxation times τ—together with

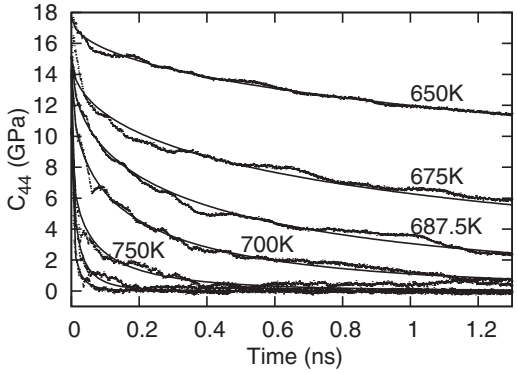

FIG. 2. Observation time dependence of the apparent shear modulus, C_{44}, obtained from an ensemble average over ≈20 independent simulation runs per temperature. The solid lines indicate fits to $C_{44}=C_{44,0}\cdot\exp(-\sqrt{t/\tau})$; the bottom two curves correspond to 800 and 850 K.

diffusion constants D; the latter had been determined by monitoring mean-square displacements in simulation cells of 3.5×10^4 atoms for ≈0.2 μs each. Both quantities clearly show a comparable behavior, which is characterized by an Arrhenius curve for temperatures lower than a critical temperature, T_C, while deviations are evident at higher temperatures. We note that for diffusivities this is well documented in experimental and simulational studies,[24] while T_C is generally regarded as the critical temperature of the mode-coupling theory[25] at which the amorphous matrix starts to appear as liquid on the time scale of individual atomic processes.

To proceed further, we employ a simple potential-energy landscape[26] picture for individual STZs [Fig. 4(a)] in which α relaxation proceeds by transitions between numerous substructured basins (reflecting the very high fragility of our model glass), while the system basically performs a random walk on the substructure.[27,28] Following Stillinger[29] we identify the latter with slow β relaxations.[30]

To rationalize our stretched exponential decay of C_{44} (Fig. 2) (Ref. 31) we first note that α events are accompanied by excessive stress fluctuations, which reduce C_{44} via F^{λ}_{ijkl} in Eq. (1) down to zero in the liquid state. While this is based on sufficient sampling of phase space, the latter is prevented in the glassy state. We cast this problem into the definition of a reaction coordinate κ [for convenience assumed to be identical for all STZs in the following (Fig. 4(a))], which needs

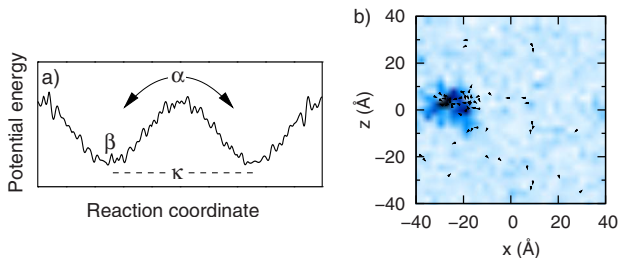

FIG. 4. (Color online) (a) Schematic model potential-energy landscape (Refs. 27 and 28) (see text). (b) Nonaffine displacement field due to uniaxial strain ($\epsilon_{22}=0.52\%$ at 10 K) in comparison with a rastered map of smallest eigenstiffnesses of the local elasticity tensors (ranging from −1831 to 21 GPa), indicating most unstable regions as shaded.

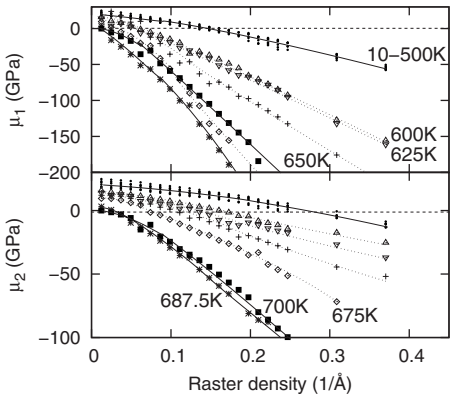

FIG. 5. Averaged smallest (μ_1) and second smallest (μ_2) eigenstiffnesses of $\tilde{C}_{ij}^{\lambda}$. The dotted lines indicate time-dependent results close to T_G, which—per se—cannot be brought to full convergence in the glassy state.

to be fully sampled to obtain liquid behavior, while only partial sampling (a fraction of $\sqrt{t/\kappa}$) occurs within time t in the glass. Assuming a uniform initial distribution in the basins along κ, and averaging over all STZs, the portion of κ, which is *not* included in the time averages, goes like $1-\exp(-\Phi\sqrt{t/\kappa})$ (with a constant Φ). This leads to a stretched exponential convergence of fluctuations and thus C_{44}.

Global viscoelastic response is clearly a consequence of processes on smaller scales; for a detailed understanding it is therefore very instructive to consider C_{ij}^{λ} on rasters of spacing, Δ, down to atomic level. For an investigation of shear stability we address the positive definiteness of C_{ij}^{λ} (viz., the positiveness of the "eigenstiffnesses" μ_m^{λ}; $m=1\ldots5$) by solving the eigenvalue problems in Kelvin notation[32] $\tilde{\epsilon}_i^{\lambda}\cdot\mu_m^{\lambda}=P_{ij}\cdot\tilde{C}_{jk}^{\lambda}/2\cdot P_{kl}\cdot\tilde{\epsilon}_l^{\lambda}$ while employing a projector, P_{ij}, to eliminate volume changes.[33] Most strikingly, at temperatures as low as 10 K more and more λ reveal mechanical instabilities with decreasing Δ (for $\Delta\lessapprox13$ Å) until ≈99% of the cells are unstable at $\Delta=2.6$ Å. Regions that aggregate mechanical instabilities are prone to yield during mechanical load, viz., to establish strain localization within STZs [Fig. 4(b)]. In fact, observations of shear localization in glassy systems date back to computer simulations by Srolovitz *et al.*[34] and have been promoted much in elaborate computational-analytical studies by Falk and Langer.[9] From a systematic analysis of the largest raster with at least one negative eigenstiffness (not shown here), the average STZ size at 10 K is readily estimated as $\approx163\pm10$ atoms, in agreement with previous results.[10,27]

For a more thorough statistical analysis of stability we sort in the following the individual eigenstiffnesses, μ_i^{λ}, in ascending order ($i=1\ldots5$) and characterize the total system with the corresponding average values, $\mu_i=\langle\mu_i^{\lambda}\rangle_{\lambda}$—as a function of raster size Δ and temperature. While the three largest averaged eigenstiffnesses, μ_3,μ_4,μ_5, remain *positive* for all temperatures investigated, it is particularly instructive to consider μ_1 and μ_2 as shown in Fig. 5; for all temperatures (even as low as 10 K) we first find that the average glass is *always* mechanically unstable on length scales smaller than ≈6.9 Å (i.e., the typical size of the short range order, as evident from μ_1), while stabilization occurs on larger scales. That is, glasses can only exist in samples exceeding a critical size which is capable of blocking all instabilities or they will spontaneously transfer into a different structure. Thus our finding therefore naturally incorporates the old notion that *frustration* (see, e.g., Ref. 2) is a key ingredient of glassy stability, which can only prevail in the presence of a sufficiently large surrounding matrix.

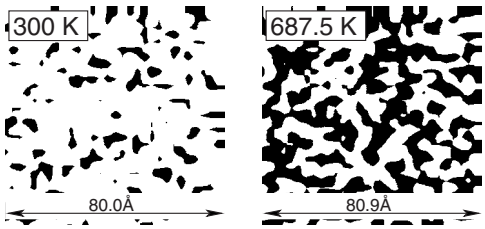

FIG. 6. Stable ($C_{44}>0$—white) and unstable ($C_{44}\leq0$—black) regions in a cross section through a three-dimensional boxed simulation cell at different temperatures on a time scale of 1 ns ($\Delta=2.6$ Å, the smallest size where each subcell contains at least one atom).

While for temperatures up to 500 K our model glass does not reveal any major changes in μ_i—in agreement with the overall mechanical response (Fig. 1)—exceeding ≈600 K results in a dramatic increase of mechanical instability in two (out of five) eigenstrain directions (Fig. 5), which is clearly to be attributed to the onset of thermally activated processes. Presumably starting from the frustration-related mechanical instabilities, the onset of thermal activations most strongly destabilizes atomic-scale configurations, affecting from there larger and larger scales, until the full cell is reached in the liquid state (Fig. 5).

Defining an overall direction of applied shear strain in an external coordinate system (e.g., ϵ_{44}), the geometry of unstable regions are readily visualized in cross-sectional plots. As evident from Fig. 6, unstable regions form a network within the cell, which appears to percolate once T_G is exceeded. In fact, as evident from the percolation correlation functions[35] calculated for the three-dimensional simulation cells (Fig. 7), the glass transition *quantitatively* appears to be a percolation transition of shear unstable region. It is inter-

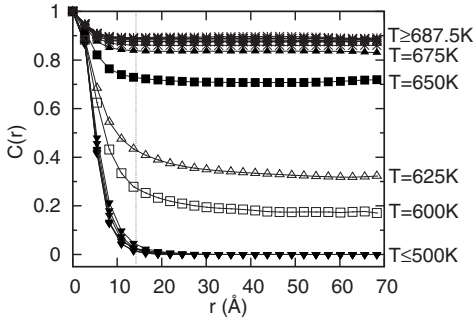

FIG. 7. Three-dimensional, azimuthally averaged site percolation correlation functions for unstable regions ($C_{ii}\leq0$, averaged over all directions $i=4,5,6$) in correspondence to the black regions in Fig. 6. The dotted line marks the approximate STZ size, as determined before (Refs. 10 and 27).

esting to point out that—prior to percolation—the correlation length of the percolation correlation function, again, reflects the STZ size.

To conclude, we have identified mechanical instabilities as key ingredients to relate structure and mechanics in glasses and supercooled liquids. Now identified, it will be very exciting to include these concepts in analytical structural models for disordered matter in the future.

It is a pleasure to acknowledge K. Samwer, W. L. Johnson, M. Zink, and M. Neudecker for valuable discussions. This research is funded by the German DFG-PAK 36.

*smayr@gwdg.de

[1] M. Born, J. Chem. Phys. **7**, 591 (1939).
[2] J. Zarzycki, *Glasses and the Vitreous State* (Cambridge University Press, Cambridge, 1982).
[3] H. Sillescu, J. Non-Cryst. Solids **243**, 81 (1999).
[4] M. Zink, K. Samwer, W. L. Johnson, and S. G. Mayr, Phys. Rev. B **74**, 012201 (2006).
[5] R. Brüning and K. Samwer, Phys. Rev. B **46**, 11318 (1992).
[6] R. Kohlrausch, Ann. Phys. Chem. **167**, 56 (1854); R. Kohlrausch, Ann. Phys. Chem. **167**, 179 (1854).
[7] A. S. Argon, Acta Metall. **27**, 47 (1979).
[8] T. Egami and D. Srolovitz, J. Phys. F: Met. Phys. **12**, 2141 (1982).
[9] M. L. Falk and J. S. Langer, Phys. Rev. E **57**, 7192 (1998).
[10] M. Zink, K. Samwer, W. L. Johnson, and S. G. Mayr, Phys. Rev. B **73**, 172203 (2006).
[11] C. A. Schuh and A. C. Lund, Nature Mater. **2**, 449 (2003).
[12] W. L. Johnson and K. Samwer, Phys. Rev. Lett. **95**, 195501 (2005).
[13] J. R. Ray, M. C. Moody, and A. Rahman, Phys. Rev. B **32**, 733 (1985).
[14] M. S. Daw and M. I. Baskes, Phys. Rev. B **29**, 6443 (1984).
[15] M. J. Sabochick and N. Q. Lam, Phys. Rev. B **43**, 5243 (1991).
[16] S. Nose, Mol. Phys. **52**, 255 (1984).
[17] W. G. Hoover, Phys. Rev. A **31**, 1695 (1985).
[18] H. J. C. Berendsen, J. P. M. Postma, W. F. van Gunsteren, A. DiNola, and J. R. Haak, J. Chem. Phys. **81**, 3684 (1984).
[19] J. F. Lutsko, J. Appl. Phys. **65**, 2991 (1989).
[20] R. J. Wolf, K. A. Mansour, M. W. Lee, and J. R. Ray, Phys. Rev. B **46**, 8027 (1992).
[21] J. F. Lutsko, J. Appl. Phys. **64**, 1152 (1988).
[22] K. Yoshimoto, T. S. Jain, K. Van Workum, P. F. Nealey, and J. J. de Pablo, Phys. Rev. Lett. **93**, 175501 (2004).
[23] Identical results can be obtained by monitoring the temporal response of shear stress upon a shear strain increment.
[24] F. Faupel, W. Frank, M. P. Macht, H. Mehrer, V. Naundorf, K. Rätzke, H. R. Schober, S. K. Sharma, and H. Teichler, Rev. Mod. Phys. **75**, 237 (2003).
[25] W. Götze and L. Sjörgen, Rep. Prog. Phys. **55**, 241 (1992).
[26] P. G. Debenedetti and F. H. Stilliger, Nature (London) **410**, 259 (2001).
[27] S. G. Mayr, Phys. Rev. Lett. **97**, 195501 (2006).
[28] J. Hachenberg and K. Samwer, J. Non-Cryst. Solids **352**, 5110 (2006).
[29] F. H. Stillinger, Science **267**, 1935 (1995).
[30] G. P. Johari and M. Goldstein, J. Chem. Phys. **53**, 2372 (1970).
[31] S. G. Mayr, (unpublished).
[32] W. Thomson, Phil. Trans. R. Soc. London **146**, 481 (1856).
[33] $P_{ij}=\delta_{ij}-Q_{ij}$ where $Q_{ij}=-1/3$ for $i,j\in(1,2,3)$; the Voigt notation treats tensor norms incorrectly.
[34] D. Srolovitz, V. Vitek, and T. Egami, Acta Metall. **31**, 335 (1983).
[35] D. Stauffer and A. Aharoni, *Perkolationstheorie* (VCH, Weinheim, 1995).